Diabetic Complications Consortium

Application Title: Modeling Diabetic Kidney Fibrosis with Kidney Organoids derived from Human Pluripotent Stem Cells

Principal Investigator: Ryuji Morizane

1. Project Accomplishments:

The support from this pilot and feasibility grant allowed me to continue my research of kidney organoids, and kidney injury and fibrosis. The proposed work has been well accomplished as a pilot study, which contributed to three manuscripts which are under review or in preparation for submission (please see the Publication section), three published manuscript, two invited review articles which are currently in preparation for submission, two invited talks, two oral presentations, and four posters at ASN kidney week 2018, several invited talks in other meetings, and NIH DP2, R01, U01, and RC2 applications which were submitted in September-November 2018. The main manuscript (Publication #2) of this proposal still requires revision and resubmission, yet I believe we achieved substantial progress in the fields of stem cells, organoids, acute kidney injury, and diabetic kidney disease. I describe the detailed results of this project in the following section.

2. Specific Aims:

Specific Aim 1: To determine whether tubular injury promotes transdifferentiation of PDGFRβ+ stromal cells into myofibroblasts and fibrosis in kidney organoids.

Results:

hPSC-derived metanephric mesenchyme cells contain stromal and nephron progenitor cells that develop into multicompartment kidney organoids which mature over time.

Kidney organoids were generated using our previously published directed differentiation protocol that subdivided mammalian kidney organogenesis into distinct intermediate stages which were chemically induced and monitored for the expression of stage-specific markers. The protocol efficiently induced SIX2+ NPCs of the metanephric mesenchyme (MM), which are multipotent cells that give rise to nephron epithelial cell types including podocytes, proximal tubules, and distal tubules. However, the MM in vivo contains SIX2-MEIS1+ stromal progenitor cells (SPCs), that differentiate into interstitial fibroblasts, pericytes, and mesangial cells (Fig. 1a). The derivatives of NPCs and SPCs organize into the distinctive architecture of the kidney cortex, noting a peritubular distribution of PDGFR-β+NG2-DESM- fibroblasts and perivascular distribution of PDGFR-β+NG2+DESM+ pericytes 38 (Fig. 1b,c). MM cells derived from hPSCs contain regions of SIX2-MEIS1+ and SIX2+MEIS1+, suggestive of SPCs and NPCs respectively (Fig. 1d). Immunostaining of SIX1 demonstrated a similar distribution of SIX2 and MEIS1 expression, consistent with overlapping SIX1 and SIX2 activity in human fetal NPCs as an auto/cross-regulatory loop drives dual expression. Concurrent flow cytometric analysis of SIX2 and MEIS1 expression confirmed the efficient induction of SIX2 (87.7 % of total cells), while nearly one quarter of the SIX2- fraction expressed MEIS1 (22.4% of SIX2- cells),

consistent with the simultaneous induction of NPCs and SPCs (Fig. 1e). Single cell RNA sequencing has revealed that human NPCs co-express stromal progenitor markers, including MEIS1 and FOXD1, unlike mouse NPCs. Our results indicate that > 99 % of hPSC-derived SIX2+ cells were positive for MEIS1, which is consistent with human embryonic kidney in vivo. The expression of FOXD1 during organoid differentiation, peaked at day 21, while a marker for interstitial fibroblasts (CD73) rises thereafter, suggesting interstitial cell maturation from an SPC pool (Fig. 1f). Meanwhile, epithelial maturation was determined by the expression of proximal tubule transcription factors found in the adult human kidney, but not present in proximal tubules of early-stage kidney organoids on single cell RNA sequencing. Significant upregulation of adult tubular transcription factors, namely BNC2, NPAS2, and TRPS1, was detected by day 50 of differentiation (Fig. 1g). Moreover, bone morphogenetic protein 7 (BMP7) expression, which governs proximal tubule cell growth and development during nephrogenesis, peaked at day 28 and was decreased by day 42 (Fig. 1h), collectively suggesting proximal tubule maturation in kidney organoids. The expression of BMP7, which counteracts TGF-β induced injury and fibrosis, suggested that organoids on differentiation day 28 or earlier may be refractory to the induction of fibrosis. Immunostaining on day 50 of differentiation revealed a stroma that is largely comprised of PDGFR-β+ cells intermixed between linear bands of ramified CD31+ endothelial cell networks, similar to the apparently normal parenchyma of adult human kidney tissue obtained from nephrectomy samples (Fig. 1i). In maturing kidney organoids, subsets of PDGFR-β+ cells co-express the pericyte markers NG2 and Desmin, as evidenced by yellow bands representing co-expression of PDGFR-β (red) and NG2 or Desmin (green) in day 50 kidney organoids (Fig 1j). Taken together, reduced expression of developmental genes and upregulated expression of adult markers was consistent with maturation of NPC and SPC regimes into multicompartment organoids, which contained the primary myofibroblast precursors of peritubular PDGFR-β+NG2-DESM- fibroblasts and perivascular PDGFR-β+NG2+DESM+ pericytes on day 50 of differentiation.

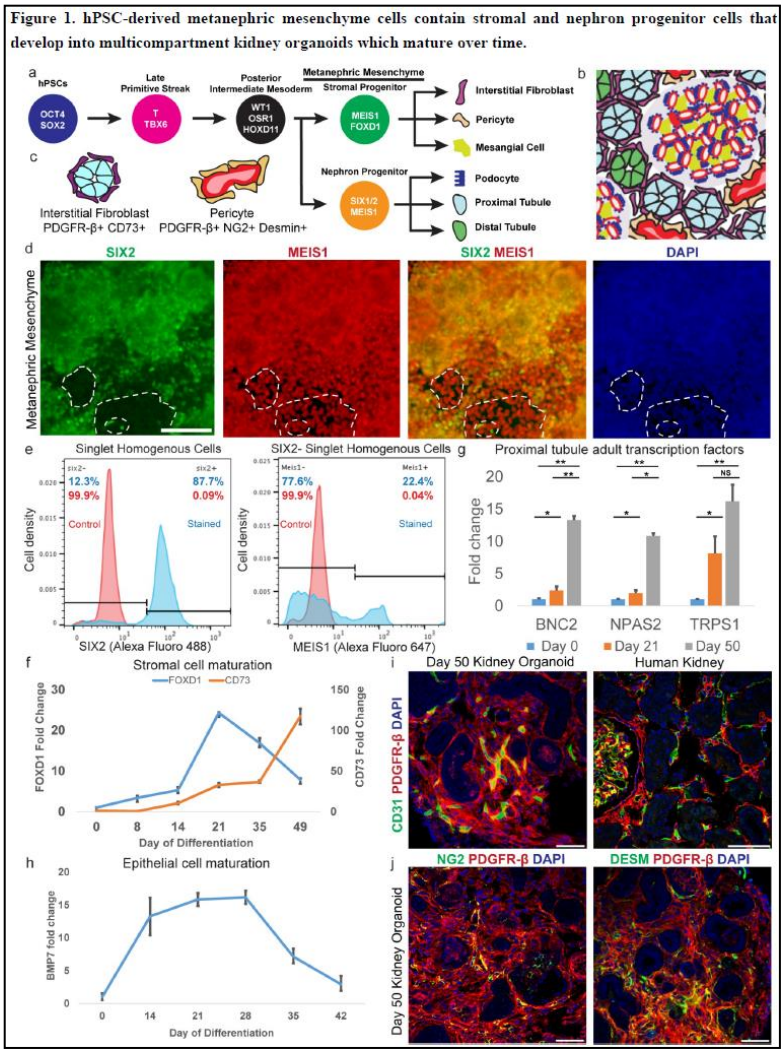

Proximal tubules in kidney organoids express transporters for cisplatin which at low concentration induces segment specific DNA damage and HR activation.

The proximal tubule aids in the excretion of cisplatin. Organic cation transporter 2 (OCT2) is one of the major transporters which mediate basolateral influx of cisplatin, which is coupled to apical efflux via multidrug and toxin extrusion proteins 1 and 2K (MATE1/MATE2K) (Fig. 2a). However, greater transport activity via OCT2 leads to intracellular cisplatin accumulation and nephrotoxicity in vivo. hPSC-derived kidney organoids express the genes of OCT2, MATE1, and MATE2K, with relatively stable expression following day 21 of differentiation (Fig. 2b). Immunostaining of OCT2 and the proximal tubule marker, lotus tetragonolobus lectin (LTL), in day 50 hPSC-derived kidney organoids appeared similar to an adult human kidney control (Fig. 2c). Treatment with low-concentration cisplatin (5 μM) induced double-stranded DNA breaks (DSBs) with expression of gamma H2A histone family member X (γH2AX) in LTL+ tubular epithelial cells, presumably mediated by the expressed transporters mimicking in vivo cisplatin pharmacokinetics, and spared podocalyxin (PODXL) and E-cadherin (CDH1) positive podocytes and distal tubules, respectively (Fig. 2d). Following cisplatin-induced acute tubular injury, ~20% of LTL+ tubular epithelial cells were positive for γH2AX, compared to <2% in negative controls. Analysis of other nephron epithelial segments demonstrated a lack of statistically significant upregulation of γH2AX in either PODXL+ or CDH1+ cells following cisplatin injury, consistent with a proximal tubule specific injury (Fig. 2e,f). Notably, LTL+ cells comprise approximately 20% of the cells in kidney organoids at day 42 of differentiation. Simultaneously with DNA damage, the proximal tubule-specific injury marker, kidney injury marker-1 (KIM-1), was manifest by greater than 83.1 ± 9.0 % of LTL+ tubular structures following cisplatin treatment, compared to 10.3 ± 5.2 % in controls. (Fig. 2e,g). Of note, quantification of KIM-1 in controls did not differ from samples stained with the secondary antibody alone used against KIM-1, consistent with non-specific brush border immunostaining. Co-staining of LTL, γH2AX and fanconi anemia complementation group D2 (FANCD2), a protein of the homology-directed repair machinery, demonstrated activation of the HR pathway to resolve DSBs in LTL+ cells treated with cisplatin (Fig. 2h,i), providing a basis that manipulation of the DDR to repair DSBs may be possible in this model system.

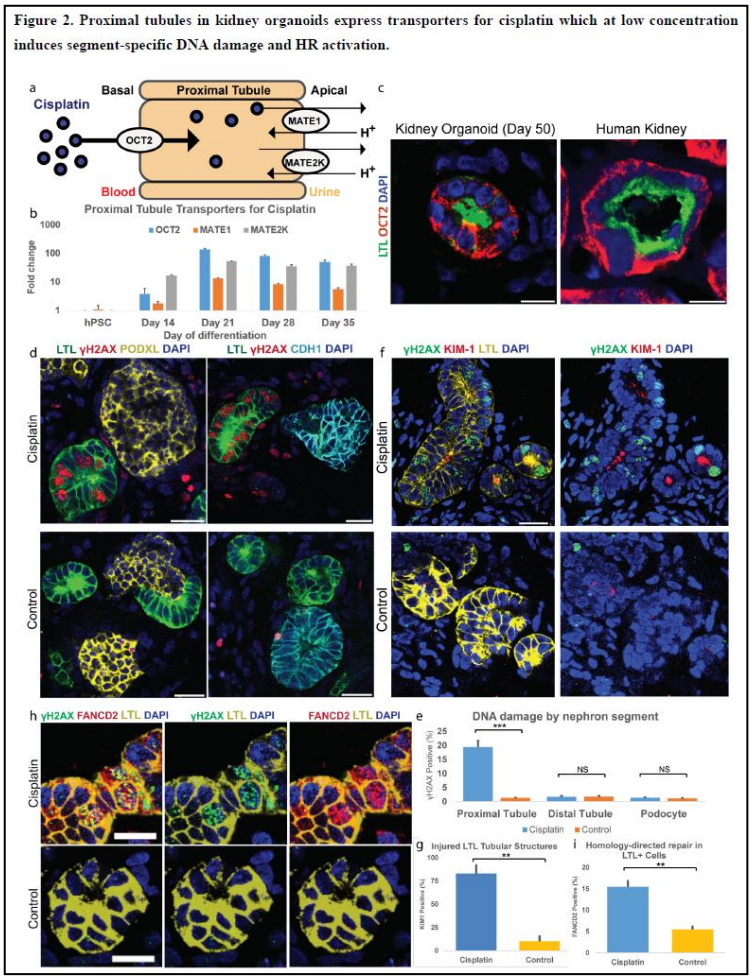

Proximal tubular cells transition from adaptive to maladaptive repair with induction of pro-fibrotic phenotypes following repeated cisplatin injury.

Kidney fibrosis is a consequence of repetitive acute kidney injury (AKI), a complication of cisplatin therapy for the treatment of solid organ tumors (i.e. head, neck, lung, ovary, testis, and breast) that occurs in 20-30% of patients. The nephrotoxicity of cisplatin is both cumulative and dose-dependent, with the proximal tubule demonstrating the greatest sensitivity to injury. Notably, repeated administration of low-dose cisplatin induces kidney fibrosis in mice. A repetitive AKI protocol, implementing low-concentration cisplatin for preferential injury to proximal tubules, was designed to model kidney fibrosis in organoids. hPSC-derived kidney organoids were subject to twice weekly cisplatin treatments from differentiation day 49 to day 64, for a total of five treatments (Fig. 3a). Early features of the tubular epithelial cells' adaptive response to injury include dedifferentiation (reactivation of tubular developmental genes), and cellular proliferation. Consistent with mammalian models in vivo, developing LTL+ tubular epithelial cells in organoids express the marker, PAX2, which is lost with proximal tubular maturation and reactivated with injury. Similar proximal tubular dedifferentiation, with induction of a kidney developmental marker, was seen with SOX9, whose activation is an early transcriptional response to AKI with descendant cells regenerating functional proximal tubular epithelium in normal epithelial repair. LTL+ cells also exhibited a mesenchymal marker, vimentin (VIM), following the initial cisplatin treatment (Fig. 3b). Notably, DNA damaged proximal tubular (LTL+γH2AX+) cells demonstrated the strongest expression of VIM, consistent with previous work that proximal tubular DNA damage induces a mesenchymal phenotype. LTL+ cells expressing Snail Family Transcriptional Repressor 1 (SNAIL1), which governs cell survival and migration, is further evidence of partial epithelial-to-mesenchymal transition (pEMT) which is implicated in progression of kidney fibrosis (Fig. 3c). Although tubular epithelial cells undergoing pEMT are not believed to directly contribute to the myofibroblast population, epithelial-derived paracrine signals such as Wnt1 promote neighboring interstitial fibrogenic cells to transdifferentiate into myofibroblasts. Notably, proximal tubular overexpression of Wnt1 implicated in tubulointerstitial feedback induced myofibroblast activation and fibrosis without leukocyte infiltration or inflammation in a mouse model, providing proof-of-concept for simulating fibrosis via induction of profibrotic phenotypes such as pEMT in proximal tubules in the model of human

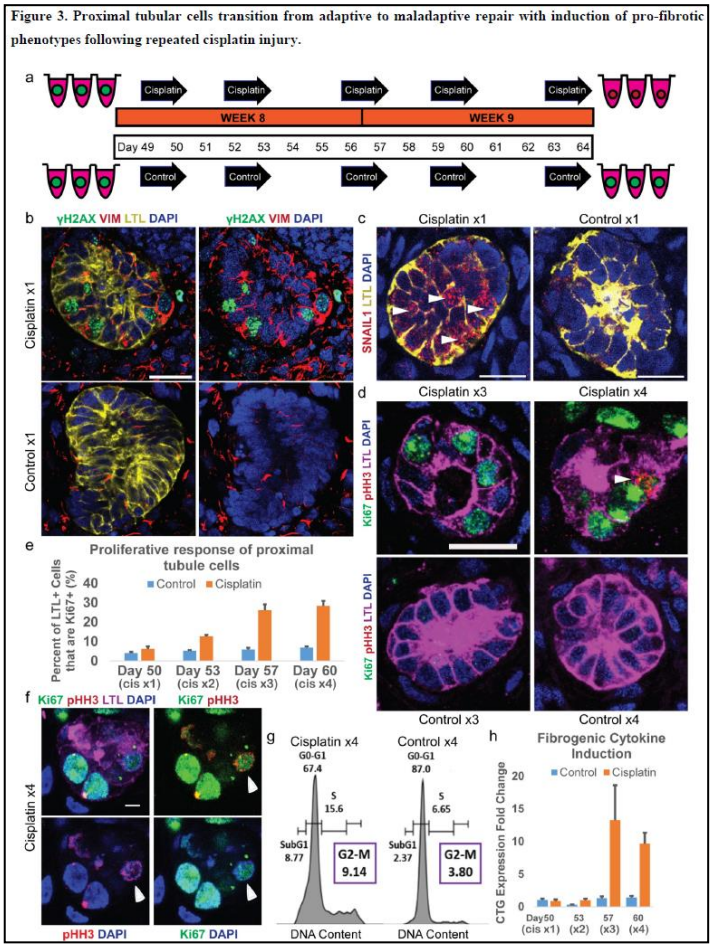

Figure 3. Proximal tubular cells transition from adaptive to maladaptive repair with induction of pro-fibrotic phenotypes following repeated cisplatin injury.

kidney organoids where inflammatory cell involvement is not apparent.

It is generally accepted that injured proximal tubular cells proliferate to replace their apoptotic counterparts and maintain tubular integrity. LTL+ tubular epithelial cells were increasingly proliferative with repeated cisplatin injury (Fig. 3d,e), with nearly 30% of the total population expressing the active cell cycle marker, Ki67, by the third cisplatin treatment. Of note, the tubular epithelial morphology starts to be disrupted after 3 times cisplatin treatment, suggestive of maladaptive tubular repair. As proximal tubular cells progress through the cell cycle, stalling or arresting in the G2/M phases is associated with a senescence associated secretory profile (SASP), including pro-inflammatory cytokine production, and interstitial fibrosis. Following the fourth cisplatin treatment, LTL+Ki67+ epithelial cells begin to manifest a speckled pattern of phospho-histone H3 (pHH3), characteristic of the late G2 phase (Fig. 3f). Flow cytometric analysis of the live LTL+ fraction for total DNA content demonstrated a 2.4-fold increase in tetraploid cells, consistent with G2/M cell cycle arrest (Fig. 3g). Correspondingly, there was increased expression of CTGF, a pro-inflammatory cytokine of the SASP and driver of fibrosis in multiple organs, including the kidney (Fig. 3h).

Repeated tubular injury induces myofibroblast activation following the conserved and divergent responses of peritubular fibroblasts in human cells.

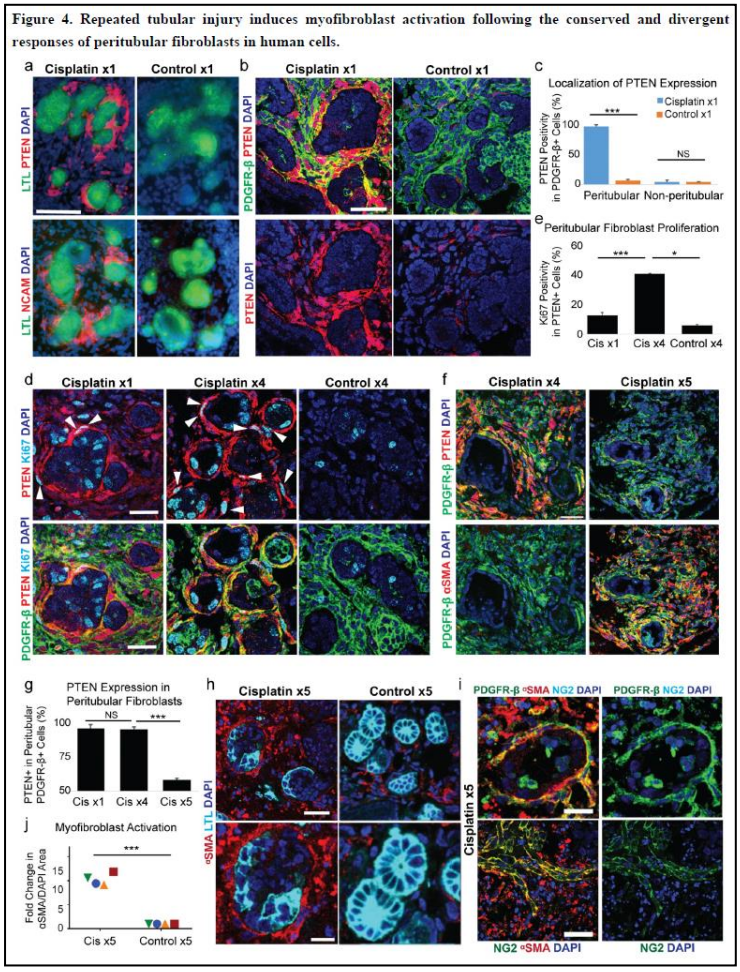

PDGFR-β+ interstitial cells develop a proliferative and migratory responses following repeated proximal tubule specific injury in vivo, prior to the advent of stromal α-SMA+ myofibroblasts and kidney fibrosis. Phosphatase and tensin homolog (PTEN), which governs cellular growth and migration by downregulating the PI3K/Akt pathway, demonstrates upregulation in peritubular interstitial cells following ischemic AKI in mice. During AKI, pharmacologic inhibition of PTEN increases TGF-β signaling, proximal tubule apoptosis, and fibrosis, suggesting that interstitial expression of PTEN may both attenuate fibrosis and promote tubular epithelial cell repair. Neural cell adhesion molecule (NCAM) is expressed in cells of the mammalian metanephric mesenchyme, however, is not expressed in the healthy adult kidney. In the human kidney, interstitial cells adopt NCAM positivity during the initial phases of the pro-fibrotic response. In a rat ischemia reperfusion injury model, NCAM+ interstitial cells

localized to the interstitium adjacent to injured proximal tubule cells during the acute injury phase. However, NCAM is expressed by proximal tubule cells in post-ischemic mouse kidneys, highlighting inter-species differences arising early in the fibrotic response. Following the initial cisplatin treatment, PDGFR-β+ interstitial cells surrounding LTL+ proximal tubule structures express PTEN and NCAM signifying reparatory and human responses, respectively (Fig. 4a,b). PTEN expression in nearly 100 % of peritubular PDGFR-β+ cells following one-time cisplatin treatment, compared to < 5% in peritubular and non-peritubular controls, suggesting that the induction of this migratory, proliferative, and reparative phenotype is a secondary effect of proximal tubule injury with cisplatin (Fig. 4c). With repeated cisplatin injury, PDGFR-β+PTEN+ cells increasingly co-express Ki67 (Fig. 4d-e), while more distant PDGFR-β+ cells continue to lack PTEN or Ki67 expression, further suggesting that interstitial cells are responding to tubular epithelial cell injury, as opposed to direct toxicity. From the fourth to the fifth cisplatin treatment, PDGFR-β+ peritubular cells transition to alpha-smooth muscle actin (αSMA)+ myofibroblast-like cells with loss of PTEN expression (Fig. 4f). During said transition, myofibroblast activation in peritubular cells is associated with a statistically significant ~2-fold reduction of PTEN expression in peritubular fibroblasts (Fig. 4g). Following the fifth cisplatin injury, the myofibroblast marker, αSMA, displayed a 10-fold upregulation by immunostaining (Fig. 4h,i). Upon further investigation, the α-SMA+PDGFR-β+ cells surrounding tubular structures lacked the pericyte marker, NG2, while non-peritubular interstitial αSMA+PDGFR-β+ cells co-expressed NG2, suggesting that peritubular fibroblasts and pericytes both serve sources of myofibroblasts (Fig. 4j).

Tubular atrophy and interstitial fibrosis correlates with an acute reduction of HR activity in DNA damaged proximal tubules.

In response to the initiation and propagation of AKI, damaged kidneys elicit an adaptive repair process to restore normal architecture. However, when the insult is severe, unremitting, or recurrent, the ensuing maladaptive repair instigates extensive ECM deposition replacing functional parenchyma. Myofibroblasts are known to be the principal matrix-producing cells, depositing interstitial fibronectin (FN) and type 1 collagen (COL1A1). Following the fifth cisplatin treatment, which is preceded by G2/M phase arrest in LTL+ tubular epithelial cells, interstitial FN deposition was upregulated by greater than 2.5-fold in kidney organoids by immunostaining, compared to untreated controls (Fig. 5a,b). Similar to α-SMA immunostaining, we observed focal FN deposition was greatest around fragmented LTL+ tubular epithelial cells (Fig. 5a bottom). Correspondingly, collagen type 1 expression revealed significant expansion of the basement membrane of injured LTL+ structures to approximately 2500 nm, compared to 900 nm in both uninjured controls and normal human kidney samples (Fig. 5c,d). Meanwhile, the COL1A1 positive area per field, standardized to nuclear area, significantly increased by greater than 50% (Fig. 5c,e). Clinically, the extent of interstitial fibrosis is commonly measured by histology, Masson trichrome (MT) staining being widely used, which demonstrated a > 3-fold increase in ECM area standardized to cross-sectional area of organoids following the fifth cisplatin treatment, as compared to untreated controls (Fig. 5f,g). Additionally, reduced organoid size and tubular atrophy were apparent on widefield views (4X) in organoid sections of maximal diameter, identified by review of serial cut sections and averaging the 2 greatest measurements for each of 3 independent organoids (Fig. 5h,i). This finding is consistent with the pathophysiology of the human kidney in vivo, in which the direct association between kidney size and tubular atrophy has been demonstrated. Analysis of human kidney tissue demonstrated

that reduced kidney function correlates with tubular epithelial and peritubular cell DNA damage, whose faithful repair is necessary for the maintenance of genomic integrity. While the proportion of LTL+ cells expressing γH2AX increased with subsequent cisplatin treatments, analysis of HR activation in the increasing γH2AX+LTL+ cellular fraction revealed a >40% reduction in FANCD2 expression between the fourth and fifth cisplatin treatments (Fig. 5j-l), which correlates with the onset of myofibroblast activation and ECM deposition. Notably, pro-inflammatory cytokines have been demonstrated to induce DNA ligase type IV, thereby promoting the error-prone, DNA repair process of NHEJ. Collectively, the association between proximal tubule atrophy, reduced HR activity, and kidney fibrosis indicates that the outlined organoid fibrotic model may serve as a platform for mechanistic analyses of tubular epithelial maladaptive repair, including impaired HR activity, for the identification of novel therapies to prevent the onset and/or progression of CKD.

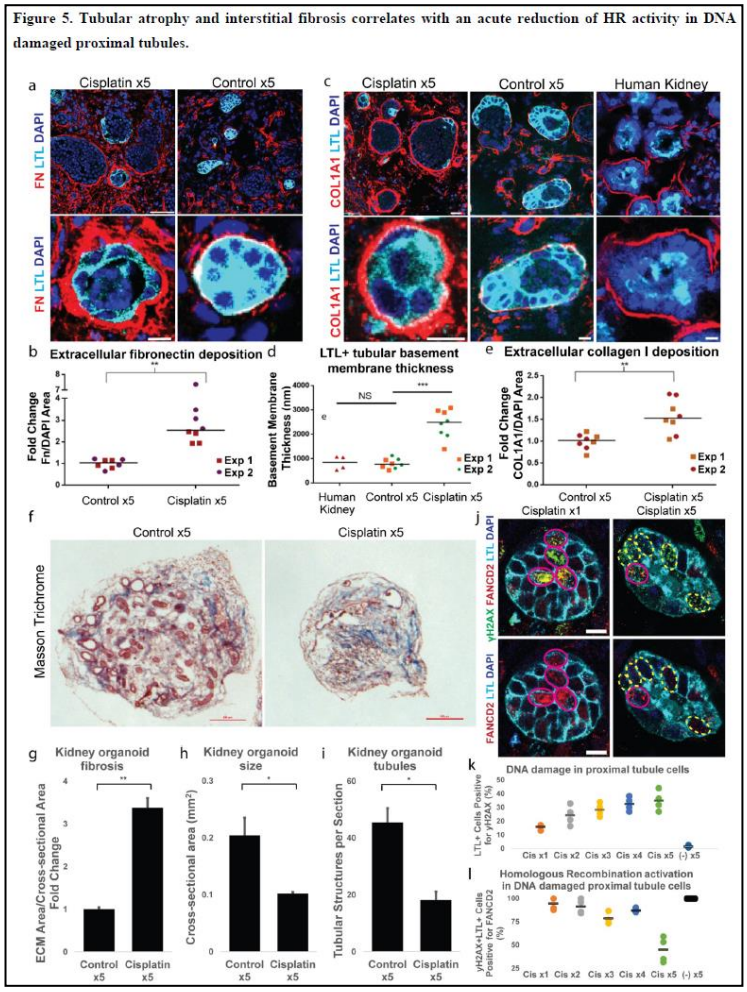

Figure 5. Tubular atrophy and interstitial fibrosis correlates with an acute reduction of HR activity in DNA damaged proximal tubules.

Inhibition of fibronectin assembly with pUR4 reduces interstitial fibrosis without affecting myofibroblast activation in response to repeated tubular injury.

Severe or recurrent tubular epithelial injury induces maladaptive repair characterized by an epithelial profibrotic phenotype, activation of myofibroblasts, and accumulation of ECM in the interstitium replacing functional tissue. The first ECM protein deposited in fibrogenesis is fibronectin, which activates integrins that serve as a chemoattractant to myofibroblasts and co-localizes with ensuing collagen type 1 deposition. However, to demonstrate cause and effect for the purpose of generating a reliable therapeutic screening platform, a fibronectin assembly inhibitor was employed and upstream and downstream processes evaluated. pUR4, derived from the F1 adhesin of streptococcus pyogenes, binds to the N-terminal region of fibronectin with high affinity and prevents fibronectin polymerization into fibrils. Continuous pUR4 was added to the repeated cisplatin-based fibrosis protocol (Fig 6a), which expectantly did not decrease myofibroblast activation (Fig. 6b,c). However, at the culmination cisplatin treatments, continuous pUR4 resulted in the total fibronectin deposition reverting to control levels (Fig. 6d,e). Notably, the accumulation of collagen type 1 matrix is regulated by fibronectin polymerization in vivo, as inhibition of fibronectin fibril formation leads to loss of collagen 1

matrix deposition. As such, the basement membrane thickness of tubular epithelial cells, by COL1A1 immunostaining, lacked a statistically significant increase compared to controls, which approximated human nephrectomy samples (Fig. 6f,g). The reported results are consistent with fibrosis in kidney organoids progressing through stages of myofibroblast activation, fibronectin interstitial deposition, and collagen type 1 accumulation, similar to human kidneys in vivo.

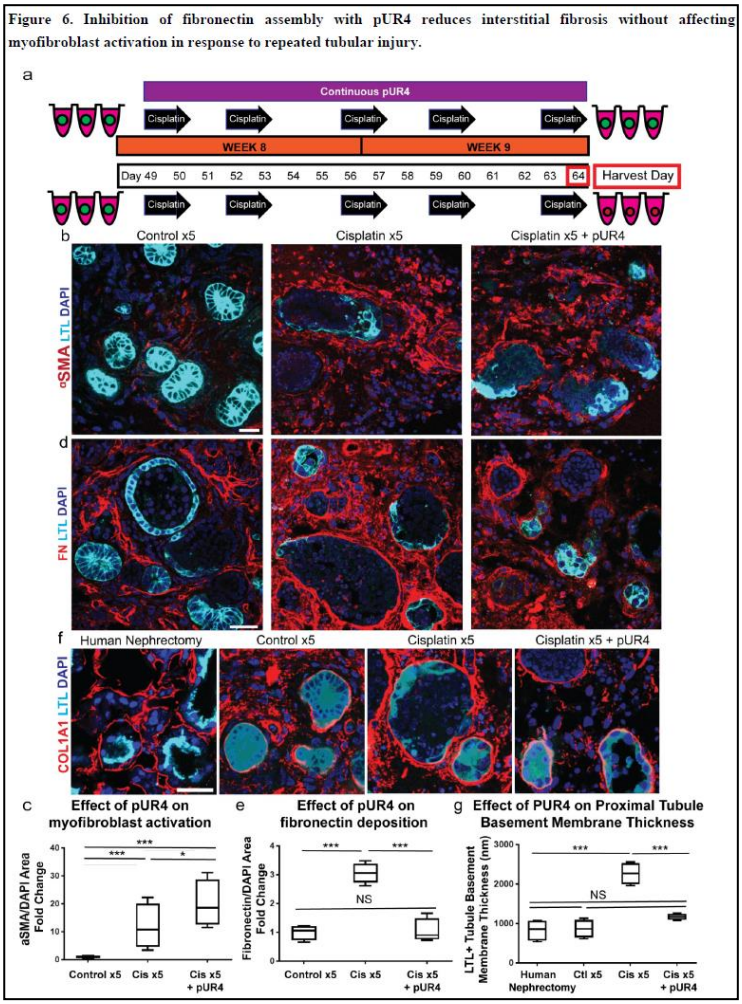

Figure 6. Inhibition of fibronectin assembly with pUR4 reduces interstitial fibrosis without affecting myofibroblast activation in response to repeated tubular injury.

Acute innate inflammatory signals hasten myofibroblast activation and interstitial fibrosis in response to repeated tubular injury.

Activation of resident macrophages and the infiltration of circulating monocytes occurs following a fibrogenic kidney injury, promoting kidney fibrosis through sustained inflammation. The macrophage-derived pro-inflammatory cytokine, interleukin 1β (IL-1β), stimulates the proliferation of cortical fibroblasts, augmenting the pool of potential myofibroblasts, and enhances deposition of interstitial fibronectin and collagen type 1. However, overexpression of pathogenic tubular epithelial cell-derived paracrine factors, characteristic of tubulointerstitial feedback, is known to induce a non-infiltrative, non-inflammatory kidney fibrosis. Moreover, the degree of kidney fibrosis is attenuated with macrophage depletion via administration of anti-macrophage serum or liposomal clodronate in ischemia reperfusion injury models. The complex milieu of pro-inflammatory and anti-inflammatory cytokines has traditionally been studied in subtractive fashion using genetic knock-out models or by overexpression or exogenous addition, possibly altering the expression of other cytokines which may be responsible for phenotypic variations. As hPSC-derived kidney organoids lack CD14+ inflammatory cells, they provide a platform for understanding the roles of singular inflammatory cell-derived cytokines in additive fashion. Following the third cisplatin injury, the addition of IL-1β 10 ng/ml during cisplatin-induced tubular epithelial injury (Fig. 7a) synergistically enhanced α-SMA expression, as compared to treatment with either cisplatin or IL-1β alone (Fig. 7b,c). Consistent with potentiated fibrosis, addition of exogenous IL-1β to cisplatin augmented the interstitial deposition of FN (Fig. 7d,e). In addition, exogenous IL-1β augmented LTL+ cell basement membrane thickness with significance compared to cisplatin x3 and IL-1β alone (Fig. 7f,g). Interestingly, as morphological disruption of LTL+ tubules was apparent with the addition

of IL-1β to cisplatin, we further analyzed DNA damage in these samples to investigate whether IL-1β exacerbates tubular epithelial injury. The addition of IL-1β to cisplatin x3 increased the percentage of LTL+ cells that were γH2AX+, while treatment with IL-1β alone was analogous to negative controls. As IL-1β did not directly injure LTL+ cells, rather synergistically enhanced cisplatin-induced DNA damage, the known stromal effects of IL-1β may contribute to tubulointerstitial feedback whereby a maladaptive repair response in peritubular fibroblasts both enhances DNA damage in injured tubular epithelial cells and promotes fibrosis. These results suggest that kidney organoids may be leveraged to evaluate the anti-fibrotic effects of novel anti-IL-1β immunotherapies currently under investigation.

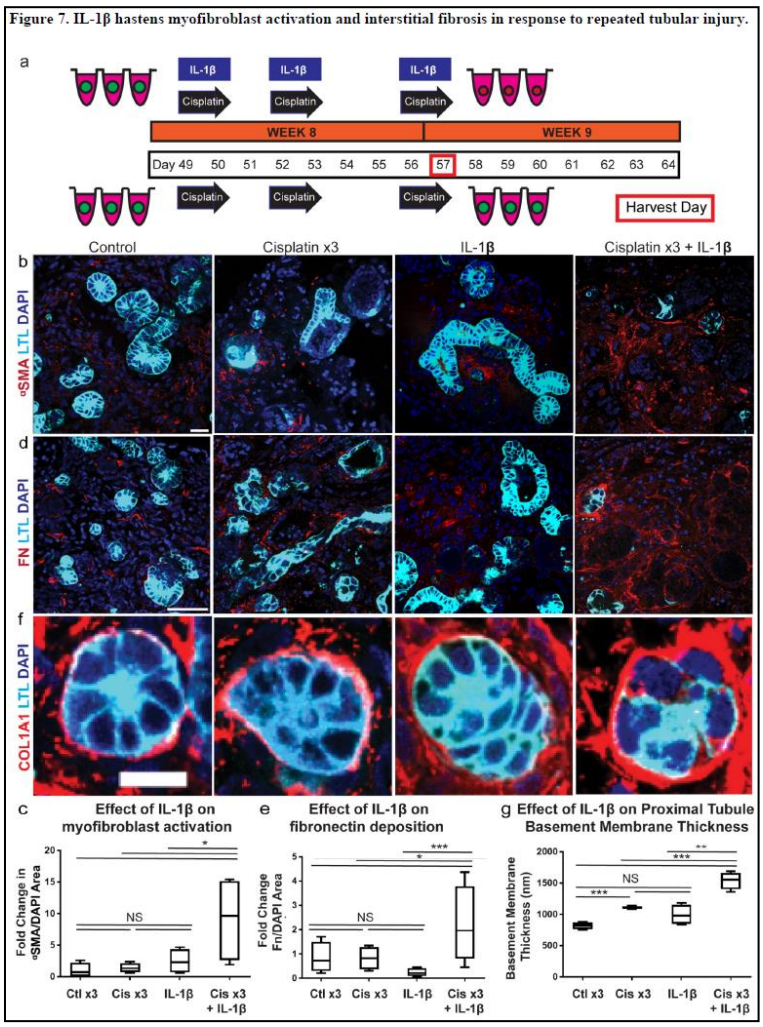

Specific Aim 2: To determine whether high glucose exacerbates the profibrotic phenotype of injured tubular epithelial cells in the presence or absence of SGLT2 inhibition.

Results:

High glucose culture facilitated α-SMA+ myofibroblast expansion and ECM deposition in kidney organoids.

Recent studies demonstrate enhanced glycolysis may cause myofibroblast transdifferentiation from kidney interstitial fibroblasts and fibrosis. First, we evaluated whether high glucose culture induces fibrotic phenotypes in kidney organoids. Kidney organoids were generated by our protocol as previously reported and cultured by day 49 of differentiation. We used the basic differentiation medium, Advanced RPMI1640, which contains 2000 mg/L glucose as control media while D-glucose was added to the basic differentiation medium to increase the glucose concentration to 4500 mg/L for high glucose culture. The organoids were cultured on 96-well plates in the control (low glucose) and high glucose media from day 49 to 69 of differentiation. Organoids were harvested for further analyses after 4 days and 20 days of high glucose culture (Fig. 8a). Immunohistochemistry of kidney organoids revealed expansion of α-SMA+ myofibroblasts-like cells in the interstitium under high glucose culture (Fig. 8b). Quantification

of α-SMA+ area/the DAPI+ count was performed using Fiji, revealing 3-fold and 8-fold increase after high glucose culture 4 and 20 days respectively (Fig. 8c). We also immunostained organoid samples for type I collagen (COL I) to evaluate extracellular matrix deposition (Fig. 8d). The COL Ⅰ-positive area in high glucose culture was increased by 1.5-fold and 2.5-fold on day 4 and 20 respectively when compared to the control (Fig. 8e). These results indicate that fibrotic lesions can be induced in kidney organoids under high glucose culture in a relatively short term, suggesting that kidney organoids may serve as a novel model to study diabetic kidney disease in human cells *in vitro*.

Figure 8. High glucose culture induces fibrotic phenotypes in kidney organoids.

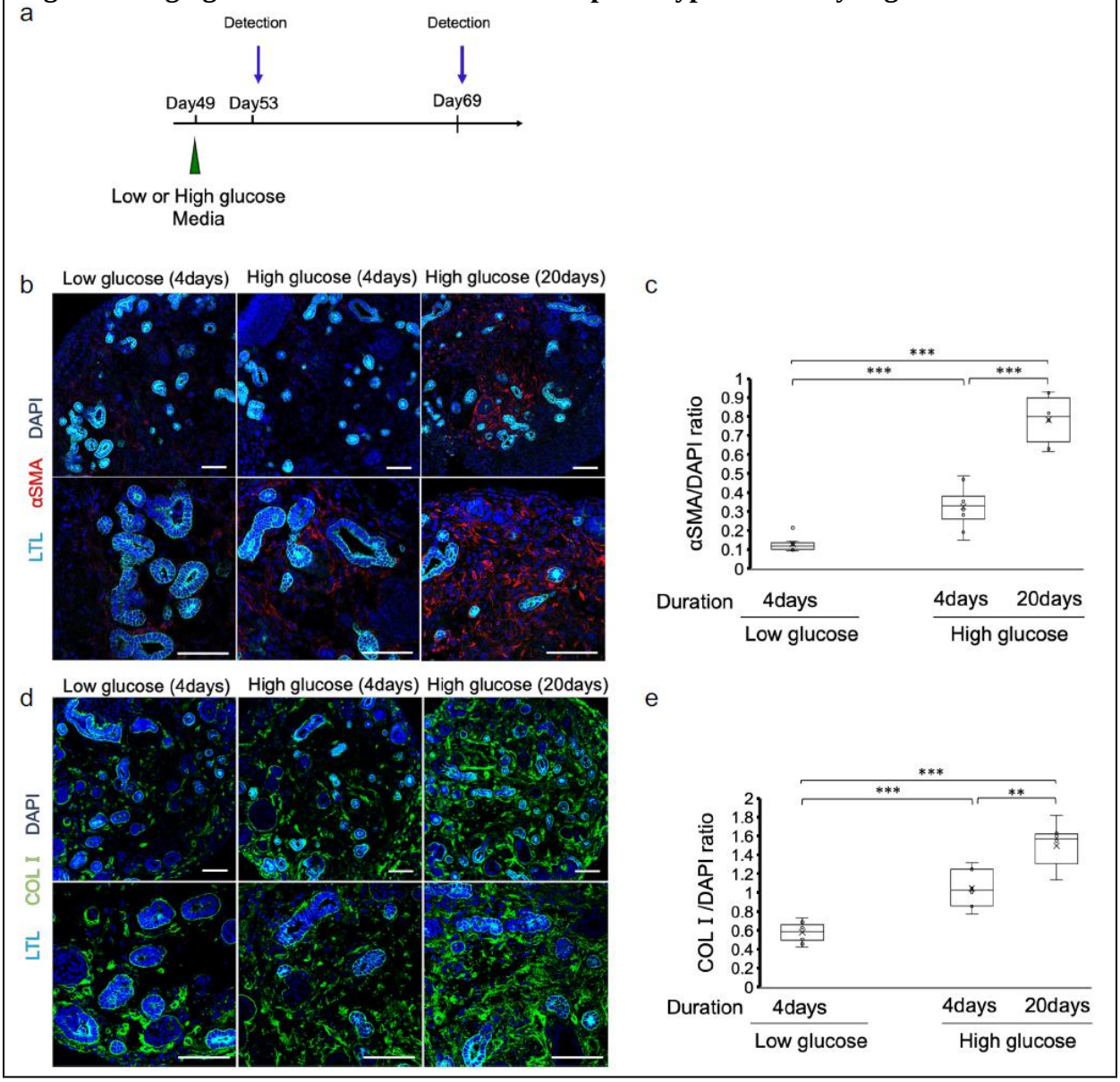

Tubular DNA damage in kidney organoids in high glucose culture and SGLT2 inhibition.

Previous studies suggest that kidney fibrosis is facilitated by multiple factors including maladaptive tubular repair and enhanced glycolysis in interstitial fibroblasts. These prompted us to explore tubular damage under the high glucose condition. Further, recent studies demonstrated that SGLT2 inhibitors may have protective effects for kidneys independently of improved blood glucose levels; therefore, we tested SGLT2 inhibition (SGLT2i) in kidney organoids. Organoids were cultured in high glucose media from day 44 of differentiation and subsequently treated with an SGLT2 inhibitor (Dapagliflozin) at 10 μM from day 46. Organoids were harvested after 9 days of high glucose culture for further analyses (Fig. 9a). To evaluate tubular injury, we immunostained organoid frozen sections for γH2AX, a marker of DNA damage, and calculated γH2AX+/LTL+ ratio. High glucose culture showed an increase tendency of γH2AX+ cells in LTL+ proximal tubular cells, and SGLT2i showed a decrease tendency of γH2AX+ cells in the high glucose condition (Fig. 9b, 9c). However, no statistical significance was observed among those samples (n=9 sections from 3 independent organoids in each condition). These results indicate that high glucose may increase DNA damage in organoid tubular cells and SGLT2i may ameliorate DNA damage. However, we concluded that we would need further experiments to confirm high glucose effects on DNA damage in tubular cells.

Figure 9. DNA damage in organoid proximal tubules treated with SGLT2i under high glucose culture.

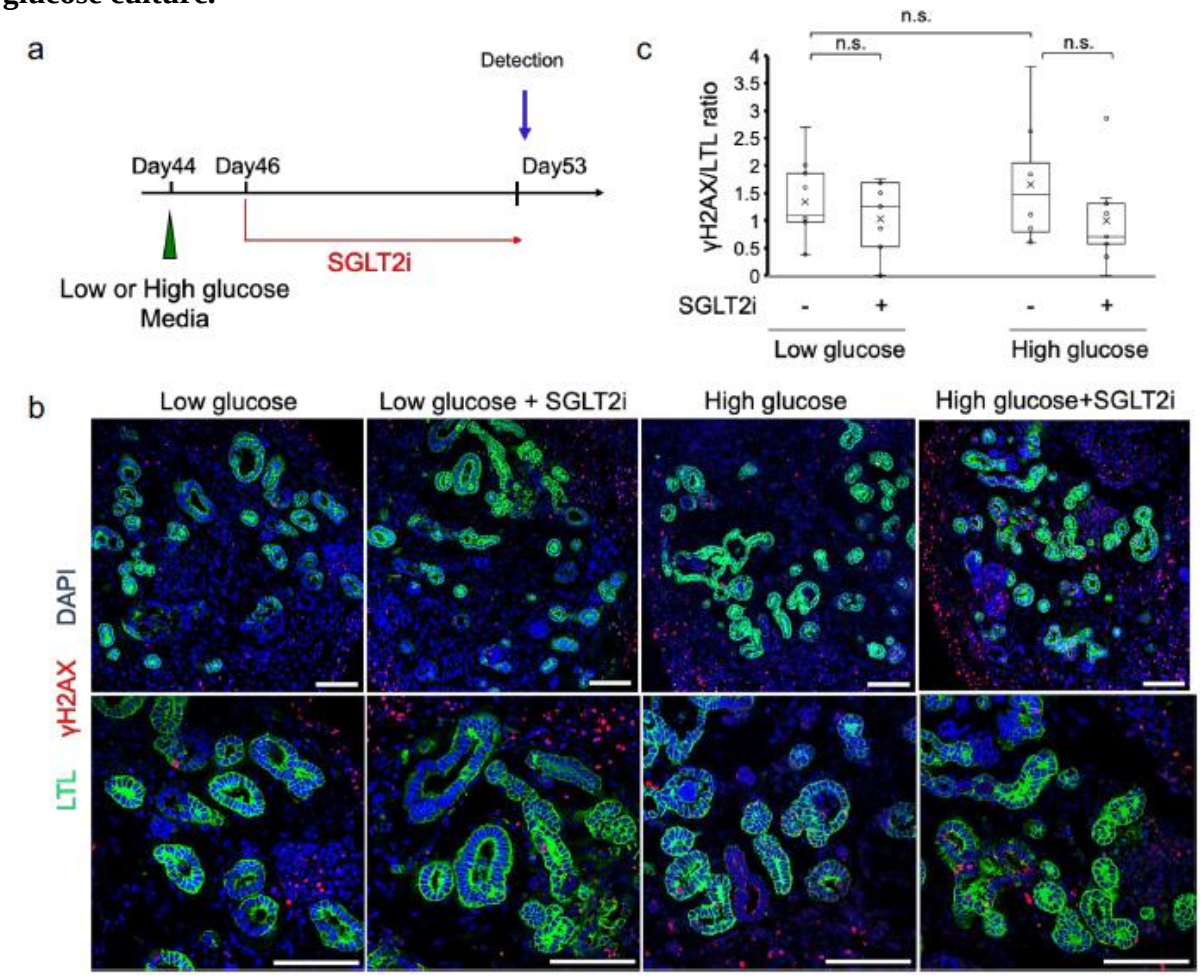

Tubular DNA damage was not enhanced by high glucose under cisplatin injury

Since we observed an increase tendency of DNA damage under high glucose culture without statistical significance, we speculated that we may observe significant difference of DNA damage in an experimental model of cisplatin-induced tubular injury. From day 44 of differentiation, organoids were cultured in high glucose media, and then 5μM cisplatin was added to media for 24 hours two times from day 49 and 52 (Fig. 10a). There was significant increase in γH2AX+ proximal tubular cells after repeated cisplatin treatment, but no additional increase of DNA damage was seen in the high glucose condition (Fig. 10b, 10c). This result may reflect the dominant effect of cisplatin which could mask the small effects of high glucose on DNA damage. We, however, concluded that tubular DNA damage may not be the dominant factor for the fibrotic change in kidney organoids under high glucose culture. Enhanced glycolysis in organoid interstitial cells may be the dominant factor for the fibrotic change. While further studies are necessary to confirm high glucose effects on DNA damage and fibrosis, this study demonstrates the utility of kidney organoids for studies of diabetic kidney disease as a novel tool.

Figure 10. DNA damage in kidney organoids treated with Cisplatin under high glucose culture.

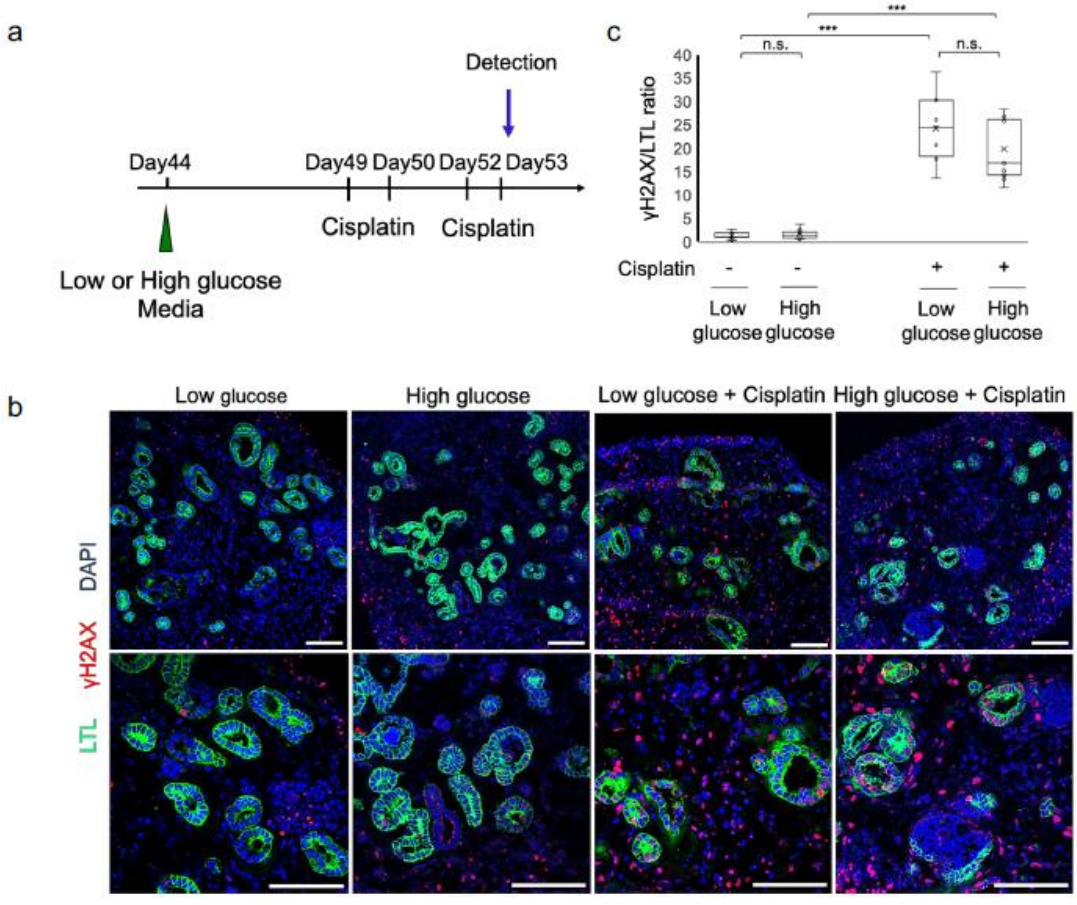

3. Publications:

1. Kimberly A. Homan, Navin Gupta (co-first authors), Katharina T. Kroll, David B. Kolesky, Mark Skylar-Scott, Tomoya Miyoshi, Donald Mau, M. Todd Valerius, Thomas Ferrante, Joseph V. Bonventre, Jennifer A. Lewis, and **Ryuji Morizane** (co-last authors). Flow-enhanced vascularization and maturation of kidney organoids *in vitro*, Nature Methods, Accepted in Principle. J.A.L and R.M are co-corresponding authors.
2. Navin Gupta, Edgar Garcia, Pierre Galichon, Tomoya Miyoshi, Koichiro Susa, Dario Lemos, Joseph V. Bonventre, Venkata Sabbisetti, **Ryuji Morizane**. Multicompartment kidney organoids model acute injury to fibrosis for therapeutic screening *in vitro*. Reviewed by three referees at Nature Medicine. In preparation for resubmission. R.M. is the corresponding author.
3. Hill SJ, Decker B, Roberts EA, Horowitz NS, Muto MG, Worley MJ Jr, Feltmate CM, Nucci MR, Swisher EM, Nguyen H, Yang C, **Morizane R**, Kochupurakkal BS, Do KT, Konstantinopoulos PA, Liu JF, Bonventre JV, Matulonis UA, Shapiro GI, Berkowitz RS, Crum CP, D'Andrea AD. Prediction of DNA Repair Inhibitor Response in Short-Term Patient-Derived Ovarian Cancer Organoids. Cancer Discov. 2018 Sep 13.
4. Gupta N, Susa K (co-first authors), Yoda Y, Bonventre JV, Valerius MT, **Morizane R** (co-last authors). CRISPR/Cas9-based Targeted Genome Editing for the Development of Monogenic Diseases Models with Human Pluripotent Stem Cells. Curr Protoc Stem Cell Biol. 2018 May;45(1):e50. R.M. is the corresponding author.
5. Lemos DR, McMurdo M, Karaca G, Wilflingseder J, Leaf IA, Gupta N, Miyoshi T, Susa K, Johnson BG, Soliman K, Wang G, **Morizane R**, Bonventre JV, Duffield JS (co-last authors). Interleukin-1β Activates a MYC-Dependent Metabolic Switch in Kidney Stromal Cells Necessary for Progressive Tubulointerstitial Fibrosis. J Am Soc Nephrol. 2018 Jun;29(6):1690-1705.

The following manuscript is in preparation for submission.

1. Koichiro Susa, Akitoshi Tamura, Pierre Galichon, Tomoya Miyoshi, Navin R. Gupta, Iman Yazdi, Joseph V. Bonventre, Sabbisetti Venkata, **Ryuji Morizane**. Kidney organoids replicate drug-induced acute kidney injury in a segment-specific manner. R.M. is the corresponding author.